

# Garnet growth in medium-pressure granulite facies metapelites from the central Damara Orogen: igneous versus metamorphic history

P. Masberg

Institut für Mineralogie, Petrologie und Kristallographie, Philipps-Universität Marburg  
35032 Marburg, Germany

The highest grade of Pan-African metamorphism in the coastal part of the central Damara Orogen culminated under lower granulite facies conditions. Thermobarometric constraints on the PT evolution of this area in migmatitic Grt-Crd-Sil-Spl-Kfs-Qtz-bearing metapelites yield an average temperature of  $725^{\circ}\text{C} \pm 16$  (locally up to  $760^{\circ}\text{C}$ ) at pressures of about 5-6 kbar. Microfabric features indicate three different generations of garnets in the metapelites. Oriented inclusion trails in garnet group I show that these garnets belong to an early syntectonic stage in the metamorphic history. Most of the garnets in the metapelites, however, occur in more or less coarse-grained leucocratic segregations. Such garnets are often anhedral and have a poikiloblastic core and an inclusion-free rim. Similar microfabric features in the leucocratic zones and their metapelitic host rocks suggest that the overwhelming part of the leucocratic segregations are products of deformation, metamorphic segregation and differentiation that outlasted annealing during regional metamorphism. It can be concluded that the garnets in these leucocratic segregations have been formed by subsolidus segregation processes prior to the peak of metamorphism. The third group of garnet is found mainly in medium-grained, migmatitic metapelites showing nebulitic structures. In such migmatites, anhedral and inclusion-bearing and euhedral inclusion-free garnets occur side by side. In contrast to garnet groups I and II, these garnets are of magmatic origin and are considered to be the products of dehydration melting of biotite at or close to peak metamorphic conditions. This high-grade metamorphic event yielded only limited amounts of *in situ* melt.

## Introduction

Microscopic features such as exsolution of mesoperthitic string perthites in alkali feldspars and antiperthites in plagioclases, oriented exsolution of rutile needles in quartz, activation of basal a and prism c glide system in quartz under conditions of plastic deformation during metamorphism indicate granulite facies metamorphism in the highest grade coastal region of the Pan-African central Damara Orogen (Masberg *et al.*, 1992). Granulite facies conditions in many regions are characterised by the appearance of orthopyroxene as a major index mineral in rocks of low-Al bulk compositions in which the isograd reaction is often ascribed to the dehydration of biotite as:



In the studied area, however, orthopyroxene is absent and the high-grade stable mineral assemblage in metapelites is plagioclase - alkali-feldspar - quartz - biotite - garnet - cordierite  $\pm$  sillimanite  $\pm$  spinel and ore, inferred to reflect the KFMASH reaction:



Previous studies of the temperature and pressure evolution of the central Damara Orogen by application of dolomite-calcite solvus thermometry yielded a temperatures increase from east to west (near Swakopmund) of around  $580^{\circ}\text{C}$  to  $645^{\circ}\text{C}$  at pressures of 2.6 to 3.4 kbar (Puhan, 1977, 1983) and  $680^{\circ}\text{C}$  at pressures of 2.5 to 3.0 kbar by evaluation of petrological data (Hartmann *et al.*, 1983). These temperature estimates, indicating amphibolite facies conditions, contradict the microscopic features noted that are present in rocks in the coastal region of the central Damara Orogen and which appear to indicate granulite facies conditions. Consequently, a re-investigation of the temperature and pressure condi-

tions during regional metamorphism was undertaken.

The studied metapelites often exhibit "core-corona-like" structures. Ashworth (1985) defined gneisses with "core-corona-like" structures in a more or less homogeneous host as flecky gneisses. In general, these structures consist of coarser grained flecks in a fine-grained matrix. Often these flecks are cored by one or more mafic minerals which are mantled by leucocratic minerals. The mafic minerals can be garnet, biotite, hornblende, magnetite etc. and the leucocratic material around them mostly quartz, plagioclase and alkali feldspar.

Two models for the formation of such segregations have been proposed by Ashworth (1985):

- partial melting or dehydration melting, and
- metamorphic segregation and differentiation.

Powell and Downes (1990) described large garnet porphyroblasts 5cm or more in diameter within leucosomes in low- to medium-pressure granulite facies metapelites in the Broken Hill area, Australia. They show that the main part of the garnet porphyroblasts occur only in the leucosome and elucidate, depending on the close similarity and close association to garnet-bearing leucosomes, that some garnet porphyroblasts without leucosome were originally enclosed within leucosome. Powell and Downes (1990) demonstrate, mainly on phase diagram considerations and pseudosections, that garnet porphyroblasts form as a consequence of incongruent melting reactions in which biotite is consumed. Unfortunately, the authors have not described in more detail the shape, the textures and the inclusion fabrics of the garnet porphyroblasts.

Similar coarse-grained leucocratic segregations are common in the studied area especially in fine- to medium-grained metamorphosed semipelites with biotite, plagioclase, quartz and only traces of sillimanite and in more Al-rich metapelites containing garnet porphyroblasts, cordierite, plagioclase, alkali-feldspar, quartz and minor sillimanite. The cores of the flecks exclusively

consist of one or more garnet crystals. Around these cores, plagioclase, quartz and alkali-feldspar form a halo free of Mg-Fe silicates. In many high-grade rocks, subsolidus deformation and recrystallisation commonly obscure anatectic microstructures. The high-grade coastal part of the central Damara Orogen is a suitable area to study microstructures of leucosomes formed by solid-state processes and of leucosomes formed by *in situ* partial melting of Al-rich metapelites because regional metamorphism, culminating in an excessive static and long-lasting high-temperature annealing, outlasted the main deformation phase.

The first aim of this paper is to present an updated data set concerning the pressure and temperature history of the studied area by the use of mineral equilibria. The second goal is, mainly based on microfabric features, to document the pattern of multiple generations of garnet porphyroblast growth within leucosomes during regional metamorphism in the central Damara Orogen.

### Geological setting and sample selection

The Damara Orogen in Namibia forms part of the Pan-African mobile belt in southern Africa and was probably formed at the triple junction of the Kalahari and the Sao Francisco Craton in Brasil during the late Precambrian to early Palaeozoic (Martin and Porada, 1977a, b). The deeply eroded Damara Orogen can be subdivided into a north-south trending coastal branch and a northeast-trending intracontinental branch which again can be subdivided into three major zones: a Northern, a Central and a Southern Zone. This subdivision is based mainly on stratigraphy, metamorphic grade and structures (Miller, 1983). The Northern Zone of the intracontinental branch was affected only by weak metamorphism and folding (Martin and Porada, 1977a). Separated by the Okavandja Lineament from the Central Zone, the Southern Zone is characterised by low- to medium-grade metamorphism with pressures of >6 kbar and a south to north increase in metamorphic grade (Hoffer, 1983). In contrast to the south-north oriented metamorphic zoning, the metamorphic grade in the Central Zone increases from east to west. Progressive metamorphism culminated in granulite facies metamorphic conditions in an area near the Atlantic coast of Namibia (Masberg *et al.*, 1992). After three phases of regional deformation, the central Damara Orogen underwent a long-lasting annealing which is documented by several microscopic features. These high-temperature conditions also led to the formation of garnet and cordierite-bearing migmatites as a result of incipient partial melting in these rocks.

The studied area is located along the west coast of Namibia. The samples were taken along a 100 km traverse from Henties Bay in the north to Rooibank in the south (Fig. 1). The rocks in the studied area belong to the Kuiseb Formation and consist of quartz-biotite schists, biotite-garnet-cordierite schists, amphibolite

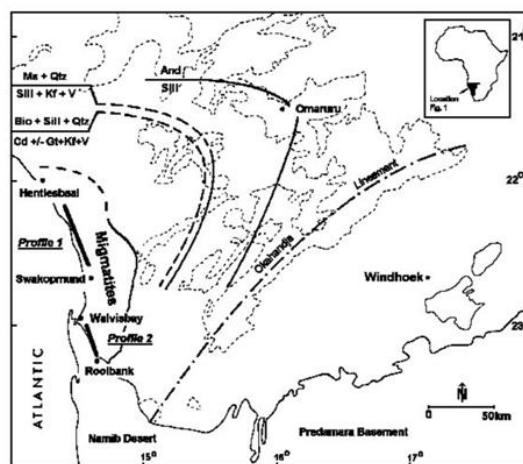


**Figure 1:** Sketch map of part of the central Damara Orogen showing the major isograd reactions worked out by Hoffer (1977, 1983) and the localities (bars) of the studied samples along two profiles near the Atlantic coast of Namibia.

schists, marbles, calc-silicate rocks and quartzites.

### Analytical techniques

Major element compositions of minerals were determined with an automated CAMECA microprobe at the University of Bonn, operating at 15kV, 20nA with a counting time of 20 s. The ZAF correction procedure was applied to the data; errors in the major oxides are estimated to be about 1-2%.

### Geothermobarometry

Metamorphic temperatures were calculated by applying the following geothermometers and calibrations: garnet-biotite, garnet-cordierite (Thompson, 1976; Holdaway and Lee, 1977; Perchuk and Lavrent'eva, 1981) and cordierite-spinel (Vielzeuf, 1983). Pressure estimates are based on the garnet-cordierite (Perchuk *et al.*, 1981), garnet-plagioclase (Newton and Haselton, 1981; Aranovich and Podlesskii, 1980) and garnet-spinel-cordierite (Harris, 1981) barometers.

A problem in determining peak metamorphic conditions is that re-equilibration is widespread in granulite facies rocks and the temperature estimates do not necessarily reflect peak metamorphic conditions because in empirically calibrated thermometers an unknown amount of re-equilibration have been incorporated into the calibrations of such geothermometers (Frost and Chacko, 1989). This re-equilibration could occur during cooling, uplift or overprinting by subsequent metamorphism. Such retrograde processes produce diffusion zonation profiles via intracrystalline diffusion. Even mineral cores no longer preserve compositions relevant to peak metamorphic conditions (Fitzsimons and Harley, 1994). Dependent on the garnet radius, the cooling rate and the ratio of garnet to biotite in the sample, these effects of post-peak re-equilibration, especially

exchange and net transfer reactions, take place in garnet-biotite mineral pairs down to 500-600°C (Spear and Florence, 1992). Further uncertainties are introduced with the choice of thermobarometers because different calibrations of the garnet-biotite geothermometer utilise different activity models for garnet and biotite. Therefore, several authors (e.g., Berman, 1988; Powell and Holland, 1985; Spear, 1993) advocated using an internally consistent set of thermobarometers resulting in more consistent estimates of temperature and pressure. A further problem in determining the metamorphic peak in the studied rocks is that the F-contents of the biotites have not been measured. These are sensitive for thermometry and the closure temperature for Fe-Mg exchange reactions between garnet and biotite. In view of

these problems, the temperatures obtained do not necessarily represent peak metamorphic conditions.

To minimise the above effects, the thermobarometric investigations were made in domains with large modal biotite contents and large garnet crystals and therefore it is very likely that the obtained temperature (garnet core-biotite) reflect near peak metamorphic conditions. Moreover, it can be assumed that under water-deficient conditions the temperatures and pressures also reflect near peak metamorphic conditions.

Metapelitic garnets in the studied samples are almandine-pyrope solid solutions with low grossular and spessartine contents (mol% almandine: 63.8 - 74.6 core, 67.6 - 76.4 rim; pyrope: 18.7 - 26.2 core 14.2 - 21.6 rim; spessartine: 3.9 - 9.7 core, 5.2 - 13.0 rim; grossu-

**Table 1:** Composition (in wt. %) of representative minerals from metapelites

Sample	40		41		65		68		70		71		187		219		246		248	
	garnet core	rim	garnet core	rim	garnet core	rim	garnet core	rim	garnet core	rim	garnet core	rim	garnet core	rim	garnet core	rim	garnet core	rim	garnet core	rim
SiO <sub>2</sub>	37.6	37.4	37.3	36.4	36.7	36.2	37.8	37.7	35.8	38.0	38.1	37.0	37.0	36.6	37.3	37.1	37.8	37.1	37.9	37.2
TiO <sub>2</sub>			0.03								0.02	0.02					0.05	0.02		
Al <sub>2</sub> O <sub>3</sub>	21.4	21.4	21.2	20.9	21.1	21.1	21.6	21.4	21.4	21.6	21.5	21.4	21.3	31.1	20.8	20.8	21.6	21.5	21.6	21.6
FeO	32.6	33.8	33.0	34.2	34.7	34.8	31.2	31.7	31.9	32.4	30.9	32.5	33.0	33.0	32.8	32.5	30.6	31.6	29.5	30.8
MnO	1.8	2.5	1.8	2.9	2.2	2.6	2.7	3.2	2.4	2.3	2.3	3.4	4.6	6.1	2.7	4.4	3.1	3.5	3.2	3.4
MgO	6.7	5.5	5.4	3.6	4.7	4.2	6.5	5.7	6.9	4.9	6.9	5.5	5.0	3.9	5.7	4.7	6.8	5.7	6.5	5.7
CaO	1.1	1.1	1.0	1.0	1.0	1.0	1.4	1.5	1.3	1.3	1.3	1.1	0.9	0.9	0.9	0.9	1.6	1.6	1.4	1.4
Sum	101.1	101.5	99.8	99.0	100.5	99.8	101.3	101.1	99.6	100.4	101.0	101.0	101.8	111.7	100.2	100.3	101.5	101.0	100.1	100.0
Alm	68.4	71.4	71.9	76.4	74.6	75.5	65.6	67.6	66.2	72.0	65.1	71.8	69.1	69.8	70.1	69.9	63.9	66.6	63.8	
Py	24.9	20.5	21.2	14.2	17.8	16.1	24.9	21.6	25.4	19.3	26.2	21.5	18.7	14.7	21.5	18.0	25.3	21.5	25.2	
Sp	3.9	5.2	4.0	6.5	4.8	5.7	5.7	6.9	5.1	5.2	5.0	4.2	9.7	13.0	5.86	9.6	6.5	7.6	7.1	
Gr	2.8	2.8	2.6	2.9	2.8	2.6	3.6	3.9	3.1	3.3	3.0	2.7	2.4	2.4	2.5	2.5	4.1	4.1	4.0	
biotite			biotite		biotite		biotite		biotite		biotite		biotite		biotite		biotite		biotite	
SiO <sub>2</sub>	34.9		35.4		35.6		36.0		35.6		35.5		34.9		35.3		36.7		36.3	
TiO <sub>2</sub>	4.3		4.7		3.0		3.3		3.4		2.1		3.2		3.6		2.2		2.9	
Al <sub>2</sub> O <sub>3</sub>	17.6		18.0		18.0		17.7		17.7		18.7		18.8		18.3		17.6		18.0	
FeO	17.9		17.9		18.3		17.3		16.9		17.8		19.1		19.4		16.4		16.9	
MnO			0.1								0.1		0.2		0.0		13.5			
MgO	11.3		10.1		10.6		12.4		12.2		12.4		11.0		10.7		0.0		12.4	
CaO																				
K <sub>2</sub> O	10.1		9.6		9.4		9.7		9.3		9.7		9.7		9.1		8.8		8.9	
Na <sub>2</sub> O	0.1		0.2		0.1		0.2		0.2		0.1		0.1		0.3		0.2		0.1	
H <sub>2</sub> O	4.0		4.0		4.0		4.0		4.1		3.8		4.0		4.0		4.0		4.0	
Sum	100.2		99.9		99.0		100.5		99.3		100.2		100.9		100.7		99.5		99.6	
plagioclase			plagioclase		plagioclase		plagioclase		plagioclase		plagioclase		plagioclase		plagioclase		plagioclase		plagioclase	
SiO <sub>2</sub>	60.7		61.2		60.1		58.4		60.2		61.1		62.6		63.1		57.2		58.2	
Al <sub>2</sub> O <sub>3</sub>	24.7		24.7		25.1		26.2		25.2		25.0		24.2		23.5		26.7		59.0	
CaO	6.1		6.0		6.6		8.0		7.2		6.0		5.1		4.4		8.4		7.7	
K <sub>2</sub> O	0.5		0.3		0.3		0.2		0.2		0.3		0.2		0.3		0.2		0.4	
Na <sub>2</sub> O	8.1		8.3		8.0		7.1		7.6		8.4		8.5		9.7		6.8		6.6	
Sum	100.0		100.4		100.1		100.0		100.4		100.9		100.5		101.0		99.4		131.9	
Ab	68.9		70.2		67.7		60.8		63.9		70.0		74.3		78.7		58.8		60.7	
Cr	2.5		1.5		1.8		1.4		1.3		1.7		1.2		1.5		1.2		1.5	
An	28.6		28.3		30.5		37.9		34.8		28.0		24.5		19.8		40.1		37.2	
cordierite							cordierite		cordierite		cordierite									
SiO <sub>2</sub>							49.1		49.1		48.4									
TiO <sub>2</sub>							0.04													
Al <sub>2</sub> O <sub>3</sub>							33.5		33.4		33.2									
FeO							7.5		7.4		8.8									
MnO							0.3		0.2		0.3									
MgO							9.5		9.8		8.9									
Na <sub>2</sub> O							0.1		0.1		0.2									
Sum							99.9		99.9		99.6									
spinel																				
Al <sub>2</sub> O <sub>3</sub>																				
Cr <sub>2</sub> O <sub>3</sub>																				
FeO																				
ZnO																				
MnO																				
MgO																				
Sum																				

lar: 2.4 - 4.1 core, 2.6 - 4.1 rim). Mineral compositions used for temperature and pressure calibrations are listed in Table 1. All investigated garnets are unzoned except for a small rim up to 30-40 mm wide where Mg decreases and Fe and Mn increase due to retrograde metamorphism. Using conventional geothermobarometry a conservative error of  $\pm 50^\circ\text{C}$  and  $\pm 1.0$  kbar should be considered (Essene, 1982). For garnet-biotite geothermometers, Chipera and Perkins (1988) and Kleemann and Reinhardt (1994) show that reasonable metamorphic temperature estimates are obtained using the calibration of Perchuk and Lavrent'eva (1981). According to these authors this specific calibration yields the most precise estimates of apparent metamorphic temperatures to within  $\pm 30^\circ\text{C}$ . The temperatures range between 704 and 759°C using garnet core compositions and adjacent biotite and between 607 and 692°C for garnet rims and adjacent biotite in which the latter are interpreted as closure temperatures for Fe-Mg exchange during retrograde metamorphism. Garnet-cordierite temperatures for core-core compositions, also using several thermometers, yield similar lower temperatures between 635°C and 726°C (Table 2).

Neglecting sample 41, pressures calculated at "peak temperatures" range between 5.9 - 6.5 kbar (Newton and Haselton, 1981) and 5.6 - 7.1 kbar (Aranovich and Podlesskii, 1980). Lower pressure estimates between 4.6 - 5.0 kbar and 4.8 kbar are obtained from garnet-cordierite equilibria (Perchuk and Lavrent'eva, 1981) and garnet-spinel-cordierite equilibria, respectively (Harris, 1981).

### Megascopic investigations

Texturally, garnets from flecky gneisses can be subdivided into three groups: syn- and post-tectonic groups related to subsolidus segregation and a group that most likely reflects dehydration melting of biotite. The first two are mostly found in the semipelitic metasedimentary rocks, the latter in more Al-rich metapelites.

The syntectonic garnet group I is represented by coarse-grained leucocratic segregations of plagioclase and quartz found in pressure shadows of garnets and in isolated fold hinges and are interpreted to be caused by extreme extension and pressure solution in an early stage of Pan-African regional metamorphism (Fig. 2). The flecks show lenticular or ellipsoidal shapes with their long axes parallel to the direction of extensional foliation of the host rock. Garnets in the cores of such flecks are poikiloblastic, anhedral and irregularly shaped. Small biotite flakes, enclosed in garnet with their long axes mostly perpendicular to the cleavage in the host rock, indicate an earlier stage of penetrative deformation. Helicitic textures indicating rotation during garnet growth are rare. Quartz grains also occur as inclusions (Fig. 3). Both the included phases exhibit finer grain sizes than matrix grains, probably due to resorption by the enclosing garnet. The included and resorbed minerals do not show any polygonal textures. The leucocratic haloes of these syntectonic flecks underwent long-lasting, high-temperature annealing under static conditions



**Figure 2:** Garnet group I bearing lenticularly and ellipsoidally shaped, coarse-grained leucocratic segregations in fine- to medium-grained semi-metapelites. The long axes of the leucocratic segregations lie parallel to the direction of extension and to the foliation of the host rock.

**Table 2:** Temperature ( $^\circ\text{C}$ ) and pressure estimates (kbar) obtained in the studied metapelites by application of the various calibrations.

Sample	40		41		65		68		70		71		187		246		248	
	core	rim																
<b>Geothermometers</b>																		
<b>garnet-biotite</b>																		
Perchuk <i>et al.</i> (1981)	750	681	706	587	724	677	712	670	756	611	737	656	698	636	696	648	706	660
<b>Perchuk und Lavrent'eva (1983)</b>	<b>750</b>	<b>690</b>	<b>712</b>	<b>607</b>	<b>734</b>	<b>692</b>	<b>723</b>	<b>687</b>	<b>759</b>	<b>632</b>	<b>742</b>	<b>670</b>	<b>704</b>	<b>650</b>	<b>712</b>	<b>670</b>	<b>717</b>	<b>677</b>
Holdaway and Lee (1977)	775	697	725	593	746	692	731	684	781	619	760	669	716	647	714	660	725	673
Thompson (1976)	831	736	770	614	795	731	778	721	838	645	812	703	760	677	757	692	770	708
<b>garnet-cordierite</b>																		
Perchuk <i>et al.</i> (1981)							695		640		710							
Holdaway and Lee (1977)							686		635		699							
Thompson (1986)							711		650		726							
<b>cordierite-spinel</b>																		
Vielzeuf (1983)											566							
<b>Geobarometers</b>																		
<b>garnet-plagioclase</b>																		
Newton and Haselton (1981)	6.4		5.4		6		6.2		6.5		6.2		6.4		6.4		5.9	
Aranovich and Podlesskii (1980)	6.2		5.1		6.7		6.9		7		6.1		5.6		7.1		6.6	
<b>garnet-cordierite</b>																		
Perchuk <i>et al.</i> (1981)							5		4.6		4.9							
<b>garnet-spinel-cordierite</b>																		
Harris (1981)											4.8							

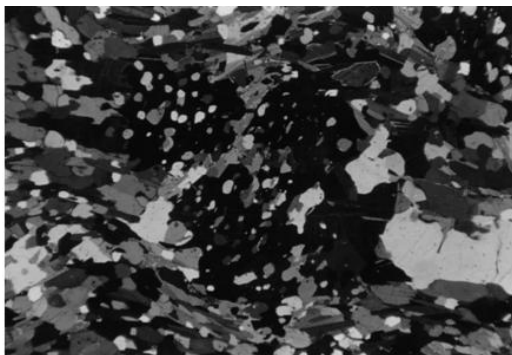


**Figure 3:** Microphotograph of the garnets in metapelites from Figure 2. Garnets show helicitic textures indicating rotation during an early stage of deformation (e.g. Passchier and Trouw, 1996). Crossed nicols. Width of the microphotograph is 0.6 mm.

leading to polygonal granoblastic or mosaic textures with well defined triple junctions and straight quartz-quartz and plagioclase-plagioclase grain boundaries.

### Garnet Group II

Most flecky gneisses in the studied area reflect a second garnet growth event. The garnets of group II grew post-tectonically in an already chemically and mineralogically differentiated rock resulting either from sedimentary layering or metamorphic differentiation. These garnet-bearing leucocratic parts occur as small bands ranging from 0.5 to 6 cm wide, as individual lenses or as more or less rounded flecks (Fig. 4). The leucocratic part consists of quartz, plagioclase and/or alkali-feldspar and accessory apatite and zircon. The mafic mineral is garnet either forming clusters of smaller crystals or a single large garnet porphyroblast. In these biotite-poor layers, quartz and plagioclase recrystallised during increasing temperature to much larger grain sizes. In the biotite-rich layers, the quartz-quartz and plagioclase-plagioclase interfaces are confined by the basal planes of biotites which strongly inhibits grain growth

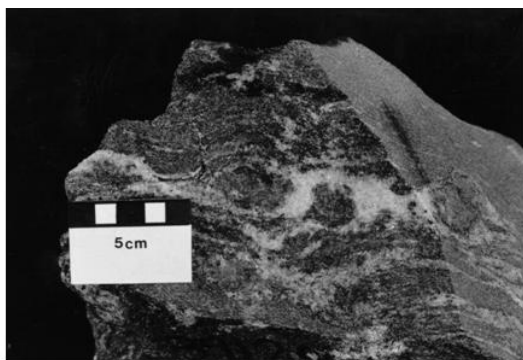


**Figure 4:** Fine- to medium-grained metapelite showing the second group of core-corona structures where big garnet crystals grew in the middle of medium-grained leucocratic segregations due to a process involving nucleation of garnet and subsequent diffusion from the surroundings under steady-state conditions.

of these minerals (Voll, 1960). Therefore the grain size of leucosome minerals is usually larger than that of the host gneiss.

The poikiloblastic garnets lie within, or grew from, the margin into the leucocratic part of the rock. They are of anhedral, rarely of euhedral shape. Sometimes garnets show an inclusion-rich core surrounded by an inclusion-free rim. Cores contain inclusions of biotite and more or less rounded quartz crystals. Enclosed quartz shows a grain size similar to that of the halo quartz due to the long-lasting annealing and grain growth after deformation. Garnet replaces quartz and also plagioclase, the latter almost completely, along the already existing and well equilibrated polygonal grain boundaries (Fig. 5). Occasionally, relicts of polygonally recrystallised quartz aggregates, which include recrystallised plagioclase with  $120^\circ$  equilibrium angles, can still be found within the garnets. This strongly indicates that garnet growth took place after recrystallisation and grain growth of quartz and plagioclase at temperatures of at least  $500\text{--}550^\circ\text{C}$  (e.g. Tullis, 1983), the lower temperature limit for collective crystallisation of plagioclase (Voll pers. comm.; Tullis, 1983). These observations indicate that group II garnets grew at higher tempera-

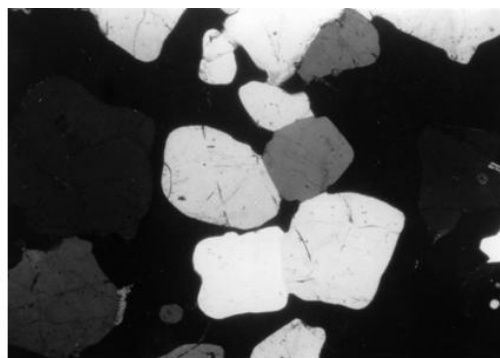


**Figure 5:** Garnet of group II replacing recrystallised quartz crystals along already existing, well equilibrated, polygonal grain boundaries. Garnet growth is determined by interfacial tension and follows high-angle boundaries between quartz grains (Voll, 1960). Due to the resorption by garnet (black) quartz grains exhibit a more or less rounded shape. Crossed nicols. Width of the microphotograph is 3.6 mm.

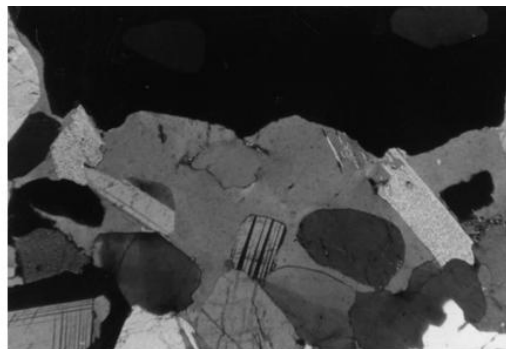


**Figure 6:** Alkali-feldspar growing as a single crystal in the interstices between subhedral plagioclases and quartz forming haloes around garnets of garnet group II. Crossed nicols. Width of the figure is 3.6mm.

tures than group I garnets.

Hence garnet has overgrown the differentiated fabric of the rock, that is the contact between biotite-rich host rock layers and the leucocratic segregation where a large change in grain size of the enclosed minerals can be seen. In the host rock, the grain size corresponds to that of the metapelitic matrix, whereas in the vein it is equivalent to the fabrics described above with polygonally recrystallised quartz and plagioclase aggregates and grain sizes are more than three times larger than the minerals in the granofelsic metapelitic host.

In some cases alkali-feldspar grew in the interstices between subhedral to anhedral plagioclase and anhedral quartz and forms haloes around garnets 1 to 2 cm in diameter. This interstitial alkali-feldspar forms optically continuous masses (Fig. 6).

### Garnet group III

The third group of garnet core-corona structures can be observed exclusively in an area just between Walvis Bay and Rooibank. In this area, garnet-biotite thermometry yield the highest metamorphic temperatures obtained in this study (760°C). The mineral composition of these Al-rich metapelites is: alkali-feldspar, plagioclase, garnet, sillimanite, cordierite, biotite, ± spinel, tourmaline and ore. Sillimanite is not present in all samples. The important mesoscopic textural feature of this group, in contrast to the features of the two other groups, is the nebulitic structure of parts of the Al-rich metapelites. Metapelitic rafts up to 5 cm in length are distorted with reference to the former structures. Such micro-xenoliths are surrounded now by a biotite-free matrix, consisting of garnet-cordierite-alkali-feldspar-plagioclase-quartz-sillimanite-spinel (Fig. 7) On the basis of shape and grain size, the garnets within these metapelites can be divided into two subgroups. Garnets of the first subgroup (IIIa) are up to 5 cm in diameter, poikiloblastic, and display core-inclusion patterns, involving mainly quartz and subordinate plagioclase, that are similar to those described for garnet group II. The outer rims of these garnets are comprised by a zone full of inclusions dominated by biotite, plagioclase, cordier-

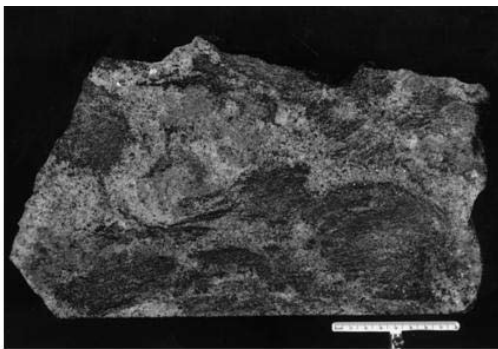


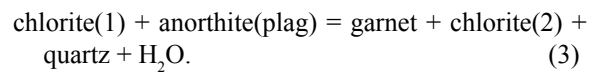
**Figure 7:** Third group of core-corona structures in Al-rich metapelites with more or less nebulitic texture. Scale bar in cm.

ite and alkali-feldspar. Replacement of quartz by garnet does not take place along polygonal grain boundaries, but in contrast both quartz and biotite exhibit irregular, often embayed shapes. The second subgroup of garnets (IIIb) are euhedral, inclusion free, and of a smaller grain size of up to 3 mm (Fig. 8). The surrounding minerals are alkali-feldspar, plagioclase and quartz.

### Discussion

The above microfabric features indicate three different generations of garnets in the metapelites. Similar mesoscopic and microscopic deformation and annealing features in the leucocratic parts and the host rock suggest that the overwhelming part of the flecks in the metapelites in the coastal area of central Damara Orogen are products of regional metamorphism and deformation. The flecks formed by subsolidus processes do not show evidence of partial melting but all of them show granoblastic polygonal textures which can be used as evidence for plastic deformation.

Inclusion trails in garnet group I show that these garnets belong to an early syntectonic stage in the metamorphic history and were probably already generated under greenschist facies conditions. According to Hoffer (1977) these early garnets may have been formed by the following reaction:



The formation of leucocratic segregations can be explained by the solution transfer of soluble minerals like quartz and plagioclase from sites of high chemical potential to those of low chemical potential for Si, Na and Ca (Gray and Durney, 1979).

Garnets of garnet group II belong to a second garnet growth event. Similar occurrences have been reported in other high-grade gneiss and migmatite terranes (Chenhall *et al.*, 1980; Tracy and Robinson, 1983;

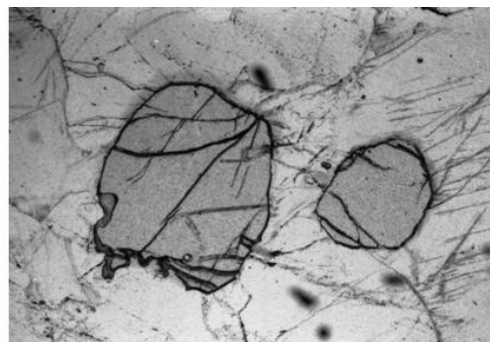
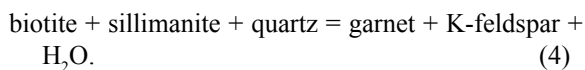


**Figure 8:** Subhedral to rounded magmatic garnets without inclusions within the granitic melt formed due to the dehydration melting of biotite according to the reaction:  $\text{Bt} + \text{Sil} + \text{Pl} + \text{Qtz} = \text{Grt} + \text{Kfs} + \text{L}$  (e.g. Le Breton and Thompson, 1988; Vielzeuf and Holloway, 1988; Patiño Douce and Johnston, 1991; Carrington and Harley, 1995). Plane light. Width of photo is 3.6 mm.

Stüwe and Powell, 1989; Jones and Brown, 1990). In metapelites from the Central Gneiss Complex in British Columbia, which are similar to the studied metapelites, such textures have been interpreted as evidence for the incongruent melting of biotite (Kenah and Hollister, 1983). As only traces of interstitial alkali-feldspar were found, these authors concluded that the majority of the melt generated must have left the rock. A major question in the investigation of Powell and Downes (1990) as to why garnet porphyroblasts are not completely retrogressed during cooling in *in situ* anatectic melts is explained by the suggestion that some disequilibrium must have been involved which can be represented by some melt loss near the peak of metamorphism. Most authors ascribe the generation of such textures to dehydration melting of biotite.

No penetrative post-metamorphic deformation has occurred in the central Damara Orogen. There is no petrographic evidence that melt has been squeezed out so that the melt migrated to adjacent dilatant sites, such as boudin necks or small dikes in unmelted protolith as described by Sawyer (1987). There is also evidence of a former melt generation has been erased as a result of subsequent high-T deformation. It can be concluded that these leucocratic segregations had already formed by subsolidus segregation processes prior to the peak of metamorphism. Furthermore, the mineral fabrics which can be observed in garnet group II are inconsistent with the process of dehydration melting of biotite because none of these flecks exhibit fabrics or mineral reaction textures that are typical of melting either within or marginal to the garnets. Thus, in analogy to mineralised quartz veins described by Masberg (1995), the replacement of existing quartz and plagioclase by optically continuous alkali-feldspar within the haloes around garnets is interpreted as a response to changing metamorphic conditions and subsolidus breakdown of biotite in the metapelites. Therefore, any material transfer between the metapelite and the leucocratic segregations around garnets must have been taken place by diffusion along grain boundaries.

Alternatively to the dehydration of biotite, the garnet formed as porphyroblasts in the unmigmatized rock and the garnet-forming reaction may have been:



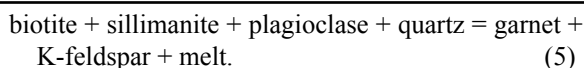
Based on mass balance calculations, Chen *et al.* (1992) suggested the same reaction for growth of garnet group II in flecked gneisses of Liuguzhuang in China. In these rocks the metamorphic temperatures were estimated to have been about 640 - 660°C and the pressures between 5-7 kbar. At these temperatures the above reaction occurs at reduced water activities ( $a_{\text{H}_2\text{O}} = 0.3$ ). The solidus curve for quartzo-feldspathic gneisses under such conditions is at about 830°C (Chen *et al.*, 1991) and such high temperatures were never reached in the

central Damara Orogen according to the available thermometry data.

For the generation of the second group of core-corona structures, a process involving the nucleation of a new phase and the diffusion from the surrounding rock volume under steady-state conditions is proposed. According to Fisher (1970, 1973), the minerals surrounding the growing nucleus will tend to disappear by reaction, changing the equilibrium to one of higher variance and megascopic segregations consisting of cores rich in the newly nucleated mineral surrounded by a mantle composed of the residue left by growth of these cores are likely to form. Once started, the nucleus continues to draw additional material from the neighbouring zone for a distance of up to several millimetres.

In contrast, garnets and leucocratic segregations of garnet group III exhibit microfabric features and mineral reaction textures related to partial melting, thus representing the only true "*in situ*" anatectic phenomena. The form of garnet growth in subgroup IIIa is interpreted to be due to dehydration melting of biotite in these samples. The garnets of subgroup IIIb are also interpreted as products of dehydration-melting reactions in which water is released from the breakdown of a hydrous mineral phase such as biotite, to enter the melt phase, leaving behind an anhydrous solid assemblage. These garnets may be peritectic or may have crystallised from the partially segregated melt. Other microscopic features within the leucosomes, such as the presence of euhedral plagioclase, euhedral alkali-feldspar with Karlsberg twins, and magmatic inclusion fabrics (small prismatic zircon crystals arranged with their long axes parallel to (110) planes of garnet) support this melting event. Similar igneous microstructures in leucosomes formed by *in situ* partial melting are reported by Vernon and Collins (1988).

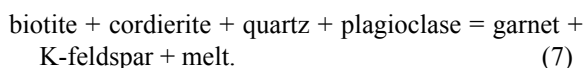
Several studies have documented that the breakdown of biotite in metasedimentary rocks results in the formation of S-type granitic melts and residual granulite facies rocks (e.g. Waters and Whales, 1984; Vernon and Collins, 1988). In addition, several experimental studies on fluid-absent melting reactions have been made with natural starting compositions to determine the temperature interval of this biotite melting reaction (Le Breton and Thompson, 1988; Vielzeuf and Holloway, 1988; Patiño Douce and Johnston, 1991; Carrington and Harley, 1995). The onset of melting is dependent on bulk composition of the rock and is further strongly controlled by the concentrations of titanium and fluorine in biotite (Carrington and Harley, 1995). Vielzeuf and Holloway (1988) showed that melting begins at 750°C and 10 kbar with a small proportion of liquid (less than 10 vol. %) and increases "dramatically" at temperatures between 850° and 862°C. In sillimanite-bearing metapelites, incipient melting according to the experiments of Le Breton and Thompson (1988) begins at pressure of about 6.5 kbar at 760°C following the reaction:



Field evidence and microscopic features show that the melt produced by this fusion event did not move far away but, locally, the removal of melt produced a quartz-deficient restite. In this restite, enclosed spinel and sillimanite in cordierite depend, according to Harley and Fitzsimons (1991), on a later partial garnet breakdown through the reaction:



According to Waters (1988) a dehydration-melting reaction of biotite in the absence of sillimanite can occur at temperature of about 750°C. For metapelitic granulites in Namaqualand he postulated the Fe-Mg continuous reaction in the system  $\text{K}_2\text{O}-\text{Na}_2\text{O}-\text{FeO}-\text{MgO}-\text{Al}_2\text{O}_3-\text{SiO}_2-\text{H}_2\text{O}$ :



In contrast to the adjacent metapelites, only traces of cordierite can be observed in the leucosomes. They are enclosed in garnet and have no direct contact with excess biotite and quartz. This indicates the cordierite consumption reaction described above. The macroscopically estimated amount of melt, produced by the two dehydration reactions of biotite does not exceed 15 vol.% in the studied metapelites.

#### *P-T-constraints for the Central Damara Orogen*

Semipelitic to pelitic metasedimentary rocks from the highest grade metamorphic part of the central Damara Orogen underwent a number of mineral reactions that monitor the P-T path of this region during the Pan-African orogenic event. The combination of thermobarometric data presented in this paper and from Jung *et al.* (1998) together with microfabric features define the conditions of peak metamorphism and part of the retrograde path of the P-T-evolution. If the amphibolite to granulite-grade reaction textures and mineral reactions described above result from a single metamorphic event, a clockwise PT path is involved. This conclusion is supported by geochronological data from the Outmoed-Migmatite-Granite-Complex (OMGC) which is situated ca. 120 km northeast of the high-grade coastal area. Here PT estimates are around 730 - 710°C and 5.1 - 5.4 kbar (Jung *et al.*, 2000a). In the OMGC, the first growth of monazite in migmatitic metapelites occurred at  $540 \pm 1$  Ma. Petrographical evidence like growth of metamorphic alkali-feldspar and cordierite with inclusions of sillimanite indicate that the country rocks were already at a high metamorphic grade at that time. The earliest granitic melts intruded only after 530 Ma. These rocks are volumetrically of minor importance.

The peak of regional metamorphism, including limited *in situ* partial melting, has been dated at around  $510 \pm 10$  Ma. Subsequently, large volumes of A-type and S-type granite intruded at about 490 and 480 Ma. These thermal events are also monitored by U/Pb monazite data and Sm/Nd garnet data (Jung *et al.*, 2000b). The features document a PT path in the Damaran crust followed in which crustal thickening is reached well before the thermal peak. Additionally, it can be inferred that the voluminous granitic magmatism is an outcome of the high thermal gradient and not the cause.

A schematic PT path for the evolution of the Central Damara Orogen is presented in Figure 9. The highest calculated temperature is about 760°C which, at the calculated pressure of 6.5 kbar, intersects the biotite dehydration reaction curve of Le Breton and Thompson (1988). Furthermore, thermobarometric results define a short isothermal decompression path at a pressure of 4.8 kbar (garnet-cordierite-spinel) at 725°C (garnet-cordierite) and 4.6 to 5.0 kbar at 650 - 700°C (garnet-cordierite). Stüwe and Powell (1989) have demonstrated that even during a small amount of decompression, cordierite reaction haloes readily form around garnet. This is in good agreement with the occurrence of cordierite coronas and quartz-cordierite symplectites around garnets (Fig. 10). According to Harley (1989), the PT path may well start with an isothermal decompression path (ITD) at  $dP/dT$  of ca. 30 bar/°C but then it evolves into a near isobaric cooling path (IBC) at  $<10$  bar/°C.

Further evidence for the clockwise PT evolution and the retrograde PT paths is the reaction postulated by Seifert and Schreyer (1970) (Fig. 11):

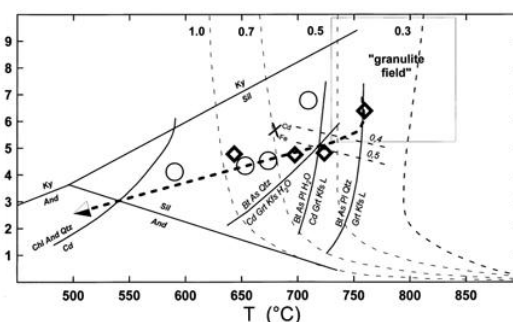
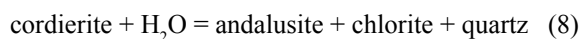


**Figure 9:** Reconstructed PT path for the high-grade central Damara Orogen along the Atlantic coast of Namibia using thermobarometric results and key mineral reactions. Diamonds represent data presented in this study, circles are data adopted from Jung (1995). Granite melting curves for several  $X_{\text{H}_2\text{O}}$  and the granulite field are from Holtz and Johannes (1994) and Johannes and Holtz (1990, 1996). Aluminosilicate triple point according to Holdaway and Mukhopadhyay (1993).  $\text{Bt}+\text{Al}+\text{Qtz} = \text{Cd}+\text{Grt}+\text{Kfs}+\text{L}$  (Holdaway and Lee, 1977);  $\text{Bt}+\text{As}+\text{Pl}+\text{H}_2\text{O} = \text{Cd}+\text{Grt}+\text{Kfs}+\text{L}$  (Harris, 1976);  $\text{Bt}+\text{As}+\text{Pl}+\text{Qtz} = \text{Grt}+\text{Kfs}+\text{L}$  (Le Breton and Thompson, 1988),  $\text{Grt}+\text{Sil}+\text{Qtz} = \text{Cd}$  for  $X_{\text{Fe}(\text{Crd})}$  at 0.4 and 0.5 (Thompson, 1976) and  $\text{Chl}+\text{And}+\text{Qtz} = \text{Crd}$  adopted from Seifert and Schreyer (1970).

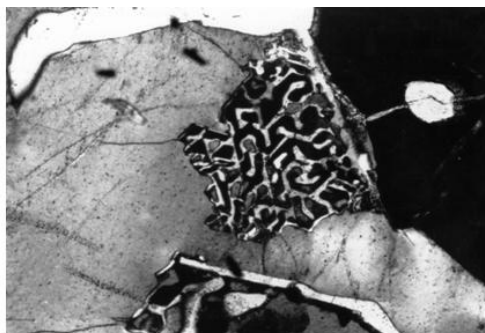


**Figure 10:** Symplectitic intergrowth between quartz and cordierite around garnet due to isothermal decompression during uplift of the Central Damara Orogen. This symplectitic intergrowth cannot be explained by a simple reaction, as  $Grt + Sil + Qtz = Crd$ ; it is possible to invoke  $Grt + L$  interaction though to help produce the  $Crd$ - $Qtz$  intergrowth (Harley, pers. comm.).

that occurs at  $P < 3-4$  kbar on cooling through temperatures of  $550^{\circ}\text{C}$ .

### Conclusions

In the coastal part of the central Damara Orogen, three genetically distinct garnet groups occur. Groups I and II belong to subsolidus formation processes during the prograde evolution of the rocks, whereas the garnets of group III were products of dehydration melting of biotite at peak metamorphic conditions. The differences in microfabric features among the two groups show that detailed textural and petrographic work is a powerful tool in distinguishing different stages in the evolution of garnets in high-grade metapelites.

Previous studies on the PT evolution of the central Damara Orogen (for review see Miller 1983) have already suggested high-grade metamorphic conditions. However, this study and several others (Masberg *et al.*, 1992, Bühn *et al.*, 1995; Jung *et al.*, 1998) indicated substantially higher conditions of metamorphism similar to other high-grade granite migmatite terranes world-wide. These new PT estimates indicate minimum metamorphic temperatures of  $760^{\circ}\text{C} \pm 50$  at pressures of  $7.0 \pm 0.5$  kbar. The limited amount of partial melt in

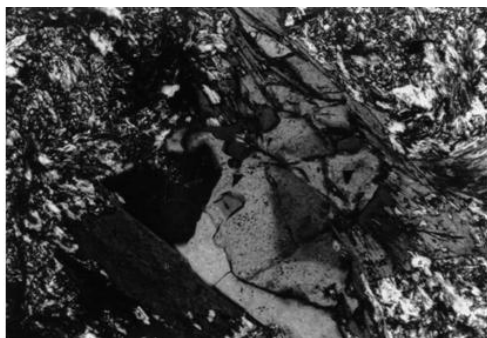


**Figure 11:** Retrograde formation of andalusite, chlorite and quartz from cordierite. Andalusite is zoned with a Mg-rich core (up to 1 wt. % MgO). Crossed nicols. Width of the microphotograph is 0.6mm.

the studied metapelites is consistent with the estimated temperatures because a high degree of partial melting requires temperatures in excess of  $800^{\circ}\text{C}$  (Clemens and Vielzeuf, 1987; Patiño Douce and Johnston, 1991; Fitzsimons, 1996). These new temperature and pressure constraints indicate, together with the dehydration melting of biotite in rocks of fertile composition and the microfabric features described by Masberg *et al.* (1992), medium-pressure lower granulite facies conditions for the western parts of the central Damara Orogen.

### Acknowledgements

I want to express my sincere thanks to Simon Harley and Johann Raith for their constructive reviews and detailed comments, which allowed me to improve the paper significantly. Any remaining errors and misconceptions in the text are entirely my own. Special thanks to Michael Raith for his kindness and generosity in allowing me to use the microprobe facility in the Mineralogical and Petrological Institute at the University of Bonn. I wish to express my thanks to Edgar Hoffer, Stephan Hoernes and Stefan Jung for stimulating discussions. The project would have been impossible without the help and the collaboration of the Geological Survey of Namibia. Financial support for these study has been provided by the German Science Foundation (Ho 1078/1-1,2).

### References

- Aranovich, L.V. and Podlesskii, K.K. 1980. Garnet-plagioclase geobarometer. *Dokl. Acad. Nauk. SSSR*, **251**, 1216-1219.
- Ashworth, J.R. 1985. *Migmatites*. Blackie and Son, Glasgow, 302 pp.
- Berman, R.G. 1988. Internally-consistent thermodynamic data for minerals in the system  $\text{Na}_2\text{O}-\text{K}_2\text{O}-\text{CaO}-\text{MgO}-\text{FeO}-\text{Fe}_2\text{O}_3-\text{Al}_2\text{O}_3-\text{SiO}_2-\text{TiO}_2-\text{H}_2\text{O}-\text{CO}_2$ . *J. Petrol.*, **29**, 445-522
- Bühn, B., Okrusch, M., Woermann, E., Lehnert, K. and Hoernes, S. 1995. Metamorphic evolution of Neoproterozoic manganese formations and their country rocks at Otjosondu, Namibia. *J. Petrol.*, **36**, 463-496.
- Carrington, D.P. and Harley, S.L. 1995. Partial melting and phase relations in high-grade metapelites: an experimental petrogenetic grid in the KFMASH system. *Contrib. Mineral. Petrol.*, **120**, 270-291.
- Clemens, J.D. and Vielzeuf, D. 1987. Constraints on melting and magma production in the crust. *Earth Planet. Sci. Lett.*, **86**, 287-306
- Chen, G., Johannes, W. and Schliestedt, M. 1991. The origin of flecked gneiss in Liuguz-Huang area, Qianan block, East Hebei, China. *Terra Abstracts*, **3**, 443.
- Chen, G., Johannes, W., Schliestedt, M. and Lan, Y.Q. 1992. The origin of flecked gneiss of Liuguzhuang

- (Qianan block, East Hebei, PR China). *Schweiz. Mineral. Petrogr. Mitt.*, **72**, 83-90.
- Chenhall, B.E., Phillips, E.R. and Gradwell, R. 1980. Spotted structures in gneiss and veins from Broken Hill, New South Wales, Australia. *Mineralog. Mag.*, **43**, 779-787.
- Chipera, S.J. and Perkins, D. 1988. Evaluation of biotite-garnet geothermometers: application of the English River subprovince, Ontario. *Contrib. Mineral. Petrol.*, **98**, 40-48.
- Essene, E.J. 1982. Geological thermometry and barometry. In: Ferry, J.M. (ed.) *Characterization of Metamorphism through Mineral Equilibria. Rev. Mineralogy*, **10**, 153-206.
- Gray, D.R. and Durney, D.W. 1979. Crenulation cleavage differentiation: implications of solution-deposition processes. *J. struct. Geol.*, **1**, 73-80.
- Fisher, G.W. 1970. The application of ionic equilibria to metamorphic differentiation: an example. *Contrib. Mineral. Petrol.*, **29**, 91-103.
- Fisher, G.W. 1973. Nonequilibrium thermodynamics as a model for diffusion-controlled metamorphic processes. *Am. J. Sci.*, **273**, 987-924.
- Fitzsimons, I.C.W. 1996. Metapelitic migmatites from Brattstarnd Bluffs, East Antarctica - metamorphism, melting and exhumation of mid crust. *J. Petrol.*, **37**, 395-414.
- Fitzsimons, I.C.W. and Harley, S.L. 1994. The influence of retrograde cation exchange on granulite P-T-estimates and a convergence technique for the recovery of peak metamorphic conditions. *J. Petrol.*, **35**, 543-576.
- Frost, B.R. and Chacko, T. 1989. The granulite uncertainty principle: Limitations on thermobarometry in granulites. *J. Geol.*, **97**, 435-450.
- Harris, N.B.W. 1976. The significance of garnet and cordierite from the Sioux Lookout region of the English River Gneiss belt, Northern Ontario. *Contrib. Mineral. Petrol.*, **55**, 91-104.
- Harris, N. 1981. The application of spinel-bearing metapelites to P/T determinations: an example from South India. *Contrib. Mineral. Petrol.*, **110**, 46-56.
- Harley, S.L. 1989. The origin of granulites: a metamorphic perspective. *Geol. Mag.*, **126**, 215-247.
- Harley, S.L. and Fitzsimons, I.C.W., 1991. Pressure-temperature evolution of metapelitic granulites in a polymetamorphic terrane: the Rauer Group, East Antarctica. *J. metam. Geol.*, **9**, 231-243
- Hartmann, O., Hoffer, E. and Haack, U. 1983. Regional metamorphism in the Damara Orogen: interaction of crustal motion and heat transfer, 233-241. In: Miller, R. McG. (ed.). *Evolution of the Damara Orogen. Spec. Publ. geol. Soc. S. Afr.*, **11**, 515 pp.
- Hoffer, E. 1977. *Petrologische Untersuchungen zur Regionalmetamorphose Al-reicher Metapelite im südlichen Damara-Orogen (Südwest-Afrika)*. Unpubl. Habilitationsschrift, Univ. Göttingen, 130 pp
- Hoffer, E. 1983. Compositional variations of minerals in metapelites involved in low- to medium-grade isograd reactions in the southern Damara-Orogen, Namibia/SW-Africa, 745-766. In: Martin, H. and Eder, F.W. (eds) *Intercontinental fold belts*. Springer, Berlin, 945 pp.
- Holdaway, M.J. and Lee, S.M. 1977. Fe-Mg cordierite stability in high-grade pelitic rocks based on experimental, theoretical and natural observations. *Contrib. Mineral. Petrol.*, **63**, 175-198.
- Holdaway, M.J. and Mukhopadhyay, B. 1993. A reevaluation of the stability relations of andalusite: thermochemical data and phase diagram for the aluminum silicates. *Am. Mineral.*, **78**, 298-315.
- Holtz, F. and Johannes, W. 1994. Maximum and minimum water contents of granitic melts: implications for chemical and physical properties and ascending magmas. *Lithos*, **32**, 149-159.
- Johannes, W. and Holtz, F. 1990. Formation and composition of H<sub>2</sub>O-undersaturated granitic melts, 87-104. In: Ashworth, J.R. and Brown, M. (eds) *High-temperature metamorphism and crustal Anatexis. Mineralog. Soc. Series*, **2**.
- Johannes, W. and Holtz, F. 1996. *Petrogenesis and experimental petrology of granitic rocks*. Springer, Berlin.
- Jones, K.A. and Brown, M. 1990. High-temperature 'clockwise' P-T-paths and melting in the development of regional migmatites: an example from southern Brittany, France. *J. metam. Geol.*, **8**, 551-578.
- Jung, S., Mezger, K., Masberg, P., Hoffer, E. and Hoernes, S. 1988. Petrology of an intrusion-related high-grade migmatite - implications for partial melting of metasedimentary rocks and leucosome-forming processes. *J. metam. Geol.*, **16**, 425-445.
- Jung, S., Hoffer, E., Masberg, P. and Hoernes, S. 1995. Geochemistry of granitic *in situ* low-melt fraction. *Communs geol. Surv. Namibia*, **10**, 21-31.
- Jung, S., Mezger, K. and Hoernes, S. 2000b. Geochronology and petrology of stromatic and reulitic migmatites from the Proterozoic Damara Belt - importance of episodic fluid-present disequilibrium melting and consequences for granite petrology. *Lithos*, **51**, 153-179.
- Jung, S., Hoernes, S. and Mezger, K. 2000a. Origin of some Pan-African syn-tectonic S-type and post-tectonic A-type granites (Namibia): products of melting of crustal sources, fractional crystallization and wall rock entrainment. *Lithos*, **50**, 259-287.
- Kenah, C. and Hollister, L.S. 1983. Anatexis in the Central Gneiss Complex, British Columbia, 142-162. In: Atherton, M.P. and Gribble, C.D. (eds) *Migmatites, melting and metamorphism*. Shiva, Nantwich.
- Kleemann, U. and Reinhardt, J. 1994. Garnet-biotite thermometry revisited: the effect of AlIV and Ti in biotite. *Eur. J. Min.*, **6**, 925-941.
- Le Breton, N. and Thompson, A. B. 1988. Fluid absent (dehydration) melting of biotite in metapelites in the

- early stages of crustal anatexis. *Contrib. Mineral. Petrol.*, **99**, 226-237.
- Martin, H. and Porada, H. 1977a. The intracratonic branch of the Damara Orogen in South West Africa. I. Discussion of geodynamic models. *Precamb. Res.*, **5**, 311-338.
- Martin, H. and Porada, H. 1977b. The intracratonic branch of the Damara Orogen in South West Africa. II. Discussion of relationships with the Pan-African mobile belt system. *Precamb. Res.*, **5**, 339-357.
- Masberg, P. 1995. Multiple migmatization in the Hat/Lp Central Damara Orogen, Namibia. *Neues Jb. Miner. Abh.*, **170**, 257-289
- Masberg, P., Hoffer, E. and Hoernes, S. 1992. Microfabrics indicating granulite-facies metamorphism in the low-pressure central Damara Orogen, Namibia. *Precamb. Res.*, **55**, 243-257.
- Miller, R. McG. 1983. The Pan-African Damara Orogen of South West Africa/Namibia. In: Miller, R. McG. (ed.) *Evolution of the Damara Orogen*. Spec. Publ. geol. Soc. S. Afr., **11**, 431-515.
- Newton, R.C. and Haselton, H.T. 1981. Thermodynamics of the garnet-plagioclase-Al<sub>2</sub>SiO<sub>5</sub>-quartz geobarometer, 131-147. In: Newton, R.C. (ed.) *Thermodynamics of Minerals and Melt*. Springer, Berlin.
- Passchier, C.W. and Trouw, R.A.J. 1996. *Microtectonics*. Springer, Berlin, 289 pp.
- Patiño Douce, A.E. and Johnston, A.D. 1991. Phase equilibria and melt productivity in the pelitic system: implications for the origin of peraluminous granitoids and aluminous granulites. *Contrib. Mineral. Petrol.*, **107**, 202-218.
- Perchuk, L.L. and Lavrent'eva, I.V., 1981. Experimental investigation of exchange equilibria in the system cordierite-garnet-biotite, 199-239. In: Saxena, S.K. (ed.) *Kinetics and equilibrium in mineral reactions*. Springer, Berlin. 273 pp.
- Powell, R. and Downes, J. 1990. Garnet porphyroblast-bearing leucosomes in metapelites: mechanisms, phase diagrams and an example from Broken Hill, Australia, 105-123. In: Ashworth, J.R. and Brown, M. (eds) *High-temperature metamorphism and crustal Anatexis*. Mineralog. Soc. Series, **2**.
- Powell R. and Holland T.J.B. 1985. An internally consistent thermodynamic dataset with uncertainties and correlations: 1. Methods and a worked example. *J. metam. Geol.*, **3**, 327-342.
- Puhan, D. 1977. Metamorphic temperature determined by means of the dolomite-calcite solvus geothermometer - examples from the central Damara Orogen (SW Africa). *Contrib. Mineral. Petrol.*, **58**, 23-28.
- Puhan, D. 1983. Metamorphism of siliceous dolomites of the central and the southern part of the Damara Orogen, 767-784. In: Martin, H. and Eder, F.W. (eds). *Intercontinental fold belts*. Springer, Berlin, 945 pp.
- Sawyer, E.W. 1987. The role of partial melting and fractional crystallization in determining discordant migmatite leucosome compositions. *J. Petrol.*, **28**, 445-473.
- Seifert, F. and Schreyer, W. 1970. Lower temperature stability limit of Mg-cordierite in the range of 1-7kbar water pressure: a redetermination. *Contrib. Mineral. Petrol.*, **27**, 225-238.
- Spear, F.S. 1993. Metamorphic phase equilibria and pressure-temperature-time paths. *Mineralog. Soc. Am., Monograph Series*, 799 pp.
- Spear, F.S. and Florence, F.P., 1992. Thermobarometry in granulites: pitfalls and new approaches. *Precamb. Res.*, **55**, 209-241.
- Stüwe, K. and Powell, R. 1989. Metamorphic segregations associated with garnet and orthopyroxene porphyroblast growth: two examples from the Larsemann Hills, East Antarctica. *Contrib. Mineral. Petrol.*, **103**, 523-530.
- Thompson, A.B. 1976. Mineral reactions in pelitic rocks: II Calibration of some P-T-X (Fe-Mg) phase relations. *Am. J. Sci.*, **276**, 425-454.
- Tracy, R.J. and Robinson, P. 1983. Acadian migmatite types in pelitic rocks of Central Massachusetts, 163-173. In: Atherton, M.P. and Gribble, C.D. (eds). *Migmatites, melting and metamorphism*. Shiva, Nantwich.
- Tullis, J.A. 1983. Deformation of feldspars, 297-323. In: Ribbe, P.H. (ed.) *Reviews in mineralogy*, 2: Feldspars (2nd ed.).
- Vernon, R.H. and Collins, W.J. 1988. Igneous microstructures in migmatites. *Geology*, **16**, 1126-1129.
- Vielzeuf, D. 1983. The spinel-quartz associations in high-grade xenoliths from Tallante (S.E. Spain) and their potential use in geothermometry and barometry. *Contrib. Mineral. Petrol.*, **82**, 301-311.
- Vielzeuf, D. and Holloway, J.R. 1988. Experimental determination of the fluid-absent melting relations in the pelitic system. Consequences for crustal differentiation. *Contrib. Mineral. Petrol.* **98**, 257-276.
- Voll, G. 1960. New works on petrofabrics. *Liverpool and Manchester geol. J.*, **2/3**, 503-567.
- Waters, D.J. 1988. Partial melting and the formation of granulite facies assemblages in Namaqualand, South Africa. *J. metam. Geol.*, **6**, 387-404.
- Waters, D.J. and Whales C.J., 1984. Dehydration melting and the granulite transition in metapelites from southern Namaqualand, S. Africa. *Contrib. Mineral. Petrol.*, **88**, 269-275.